



## AERODYNAMIC DESIGN AND DETERMINATION OF PERFORMANCE CURVES THROUGH CFD TECHNICALS OF AXIAL ROTOR OF REVERSIBLE JET FAN

**Angie Lizeth Espinosa Sarmiento**

**Waldir de Oliveira**

Universidade Federal de Itajubá, Av. BPS 1303, Pinheirinho, Itajubá, MG, Brazil  
angieespinosa.sar@gmail.com  
waldir@unifei.edu.br

**Ramiro Gustavo Ramírez Camacho**

Universidade Federal de Itajubá, Av. BPS 1303, Pinheirinho, Itajubá, MG, Brazil  
ramirez@unifei.edu.br

**Yina Faizully Quintero Gamboa**

Universidade Federal de Itajubá, Av. BPS 1303, Pinheirinho, Itajubá, MG, Brazil  
yinafaizullyquintero@gmail.com

**Abstract.** *The main feature of a Reversible jet fan is to provide the same air flow and thrust in both directions of flow, keeping the maximum ratio thrust-power in any range of electrical motor power. These conditions could be achieved with the use of a rotor formed by double-symmetric airfoils, for example, an elliptical airfoil. This paper present a rotor blade design of a reversible axial rotor of a jet fan usually used for ventilation of road tunnels, the design is based on a methodology that utilizes a non-free vortex condition for resolving the radial equilibrium equation. This project was developed with reference in certain data available in the literature of elliptical profiles arranged in linear cascades representing axial rotors, gotten by means of computational fluid dynamics tools. Moreover, the characteristics of aerodynamic performance of the reversible axial rotor were found either in the design point or out of this for a specific rotation using Computational Fluid Dynamics Methods (CFD) by means of the commercial software Fluent®. With numerical simulation results is possible to plot the fan performance curves, total pressure and fan's shaft power which show good agreement respect to the design data.*

**Keywords:** *Reversible jet fan, axial-flow fan, rotor blade design, non-free vortex, Computational Fluid Dynamic, Fan performance curves.*

### 1. INTRODUCTION

The jet fans are commonly used in road tunnel ventilation relatively short lengths, usually less than 5 km. Banks of these fans are installed in the roof of the tunnel at certain intervals, thereby producing an effective flow of air from one side of the tunnel to the other. By saving energy, jet fans operate when the air quality deteriorates enough to require the forced ventilation assistance. The jet fans for longitudinal ventilation of road tunnels are fans of axial type. The rotor of this type of fan has a low hub ratio (ratio between the inner diameter and the outer diameter of the rotor). Generally, the hub ratio for this sort of rotors is in the range 0.3 to 0.4. Consequently, these have high specific rotations characterized by high flow rates and low pressures. The blades number of these rotors is usually between 5 and 12, depending on the performance characteristics and of aerodynamic noise required. With the aim of varying the speed of the air jet, and accordingly the thrust produced by the fan, the blades are attached to the hub of the rotor, so that the mounting angle can be adjusted in the desired position.

Relative to the flow direction of jet fans are classified into two types: unidirectional and bidirectional, the latter also being known as reversible. The unidirectional type is most appropriate for the longitudinal tunnel's ventilation in a single direction of vehicular traffic; because its reversion (direction reversion of rotation of the rotor) results in 50 to 60% of the thrust in the direction of normal rotation. Each radial section, along the blades of this type of fan is generally made with a curved airfoil having different leading edge and leading trailing. The high performance achieved in these fans, is the result of the geometric characteristics of the blades with that kind of profile and consequently, higher thrusts are obtained when are compared with the reversible jet fans. Therefore, reversing the direction of rotation and consequent reversion of flow direction in unidirectional fans, causes a drastic reduction in aerodynamic performance characteristics.

In the case of reversible jet fans, the blades are formed by symmetrical profiles in all radial sections thereof. Such profiles can have format in "S" or any other format without cambering that present bidirectional symmetry (symmetry with respect to the chord line and in relation to the line perpendicular to the midline of the cord) as the elliptical profile. These geometric characteristics of the blade are responsible of the low performance and thrusts compared with the

unidirectional jet fans. Regarding the reversible jet fans, there are few jobs available in the literature. In the sequel some relevant works are commented.

Köktürk (2005) presents an aerodynamic design methodology for reversible axial fans. This methodology uses the results of cascades analyses of axial flow machine, through computational fluid dynamics (CFD), using the commercial software Fluent ®. All analyzed linear cascades are formed by elliptical profiles with maximum aspect ratio of 8% of the length of his chord. For each angle of attack, the author varied incidence speed and blade spacing. In this study, were also obtained aerodynamic performance characteristics of axial rotor, concluding that maximum efficiency is not achieved at the point of design, but at a point very close to this.

In the work of Santolaria. *et al.*, 1996 is presented the aerodynamic design, construction, test procedure and test results aerodynamic and of noise of a reversible jet fan for road tunnels. The authors do not present the methodology rotor aerodynamic design; expose only two projections of blades formed by elliptical profiles, indicating simply the polar radius dimensions of each one the 10 radial sections. Was concluded that the aerodynamic performance of the fan was quite satisfactory, however, the fan emitted a high power sound by virtue of the high speed of movement within, and the uniformity lack of the air flow, associated with the simplified construction of fan, due it was not used an appropriate acoustic insulation.

In the paper of Ballesteros *et al.*, 2002 was carried out a numerical and experimental study of air circulation inside of a reversible jet fan, whose rotor had blades formed with elliptical profiles, to provide the same pressure in both directions of operation. In this analysis was used the commercial software Fluent ®. In the experiments were obtained radial distributions of the static pressure, total pressure and of the different velocity components in different sections of the fan, agreeing numerical and experimental results. In this work the authors seek to obtain a tool to facilitate the design and improve the development of new fans, also observe the flow behavior in inaccessible areas in laboratory tests. It is worth mentioning that the last two works were conducted by researchers at the University of Oviedo, Gijón, Spain. In this city, is located the Zitron matrix, a leading manufacturer of various types of fans.

Thus, the main objective of this paper is to analyze the aerodynamic performance characteristics of reversible axial-flow rotors of jet fan obtained in preliminary studies, in order to optimize this type of machine for certain operating conditions.

## 2. DESIGN METHODOLOGY

This section features, initially, the main geometric quantities of the rotor. Next, the methodology of aerodynamic design for the reversible axial rotor is presented.

### 2.1 Main geometrical quantities of the reversible axial rotor

To obtain the rotor flow,  $Q$ , is necessary to carry out an iterative procedure (Espinosa, *et al.*, 2011) which is fixed outside diameter of the rotor,  $D_e$ . Therefore, it must be checked if  $D_e$  agrees with the axial rotors optimized for the set of values of rotational speed,  $n$ , flow,  $Q$  and total pressure  $\Delta p_T$  corresponding to the point of optimum performance (max) rotor. The diameter  $D_e$  can be obtained by the coefficient diameter,  $\delta$ , through of Cordier type graphs that relate the lightness coefficient,  $\sigma$ , whit  $\delta$ , (Cordier, 1955). Expression of  $\sigma$  and  $\delta$  are given in the Eq. (1) and Eq. (2).

$$\sigma = 2^{1/4} \pi^{1/2} \frac{Q^{1/2}}{(\Delta p_T / \rho)^{3/4}} n \quad (1)$$

$$\delta = \frac{\pi^{1/2} (\Delta p_T / \rho)^{1/4}}{2^{3/4} Q^{1/2}} D_e \quad (2)$$

A graph correlating  $\sigma$  with  $\delta$ , specific for axial rotors of low ratios of hub, typical of rotors of fan jet, is shown in Eck (1973). Based on this graph,  $\delta$  and  $\sigma$  can be correlated by Eq. (3).

$$\delta = 1,4678 - 0,7081 (\ln \sigma) + 0,4158 (\ln \sigma)^2 - 0,1424 (\ln \sigma)^3 \quad (3)$$

After obtaining  $\delta$  by Eq. (3), and considering the Eq. (2), the outer diameter of the rotor,  $D_e$ , is calculated by Eq. (4).

$$D_e = \frac{2^{3/4}}{\pi^{1/2}} \frac{Q^{1/2}}{(\Delta p_T / \rho)^{1/4}} \delta \quad (4)$$

The hub diameter of the rotor,  $D_i$ , generally, is determined by the hub ratio,  $v = D_i/D_e$ , which can be obtained from specific graphics. Eck (1973) provides a minimal hub ratio for various installations of rotors and of axial fans. In the case of axial rotor of jet fans,  $D_i$  is determined by the outer diameter of the housing of the electric motor,  $D_{car}$ . Once established the shaft power,  $P_e$ , rotational speed,  $n$  and the type of fixation of the electric motor,  $D_i$  should be slightly higher or at least equal to  $D_{car}$ . Thus,

$$D_i \geq D_{car} \quad (5)$$

Known  $D_i$  and  $D_e$ , the hub ratio,  $v$ , is determined by Eq. (6).

$$v = \frac{D_i}{D_e} \quad (6)$$

The ratio hub should not be less than that recommended by Eck (1973). Another important geometric quantity is the number of rotor blades,  $N_{pá}$ . In jet fans, the number of rotor blades is usually established according to Eq. (7) Bleier (1998).

$$N_{pá} = 5 \text{ to } 12 \quad (7)$$

## 2.2 Aerodynamic design of reversible axial rotor

In the solution of radial equilibrium equation (equation of momentum in the radial direction) are adopted, certain types of non-free vortex, for example, Yahya (1983), for design of the blades. In these methods, both the specific work of the rotor,  $Y_{pá}$ , and meridional velocity,  $c_m$ , are no longer constant along the length of the rotor blades. In this paper is used, a type of non-free vortex adopted by Wallis (1993), where the circumferential component of the absolute velocity after rotor,  $c_{u6}$ , varies linearly along the blade. This condition is represented of dimensionless form by Eq. (8).

$$\varepsilon_6 = \frac{c_{u6}}{\bar{c}_m} = a + bx \quad (8)$$

where  $\varepsilon_6$  is the swirl coefficient at the exit of the blades,  $\bar{c}_m$  the mean meridional velocity along the blade,  $x = r/r_e$  the ratio of a given radius  $r$  and the outer radius  $r_e$ , with  $r$  between the hub radius  $r_i$  and outer radius  $r_e$ , and  $a$  and  $b$  constants to be determined.

The main reason for choosing the condition of non-free vortex represented in the Eq. (8) is due to the fact of to work with hub ratios,  $v$ , relatively low, which are typical of jet fans. For these fans, the hub diameter,  $D_i = 2r_i$ , generally, is considered equal to the outer diameter of the housing of the electric motor that directly drives the rotor. Therefore, for certain thrust produced by the jet fan will result an electric motor with shaft power, rotational speed and defined housing, and also a defined outer diameter of the rotor, resulting in hub ratios with values generally lower than 0.4. For these hub ratios, if is used free-vortex condition would results in inefficient rotor and presents a strong twist of the blades in the region close to the hub of the rotor, thereby influencing the characteristics of aerodynamic performance.

The approximate solution of the equation of momentum along the blade, considering that no swirl of the flow at the inlet of the rotor (pre-rotation), that is, the circumferential component of the absolute velocity at the inlet,  $c_{u3} = 0$ , Fig. 1, can be obtained by (Wallis, 1993):

$$\left(\frac{c_{m6}}{\bar{c}_m}\right)^2 = \left(\frac{c_{m3}}{\bar{c}_m}\right)^2 + \left[\varepsilon_6 \left(\frac{2}{\phi} - \varepsilon_6\right)\right] - \left[\varepsilon_6 \left(\frac{2}{\phi} - \varepsilon_6\right)\right]_{\bar{x}} - 2 \int_{\bar{x}}^x \varepsilon_6^2 \frac{dx}{x} \quad (9)$$

where  $c_{m6}$  is the meridional component of the absolute velocity at the exit,  $c_{m3}$  is the meridional component of the absolute velocity at the inlet and  $\phi$  is the flow coefficient defined by Eq. (10).

$$\phi = \frac{c_m}{\bar{c}_m} \quad (10)$$

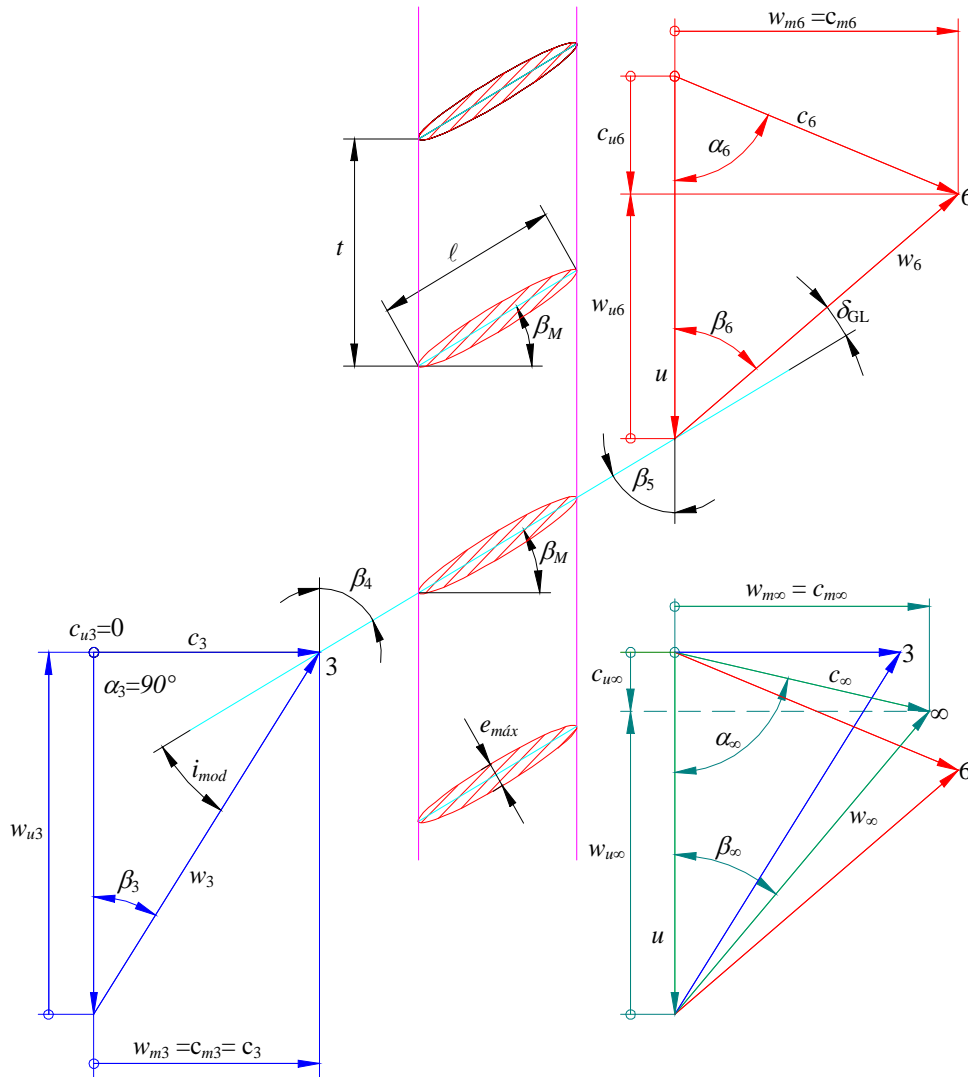


Figure 1. Representative linear cascade of a radial section of reversible axial rotor indicating only one direction of flow

In the Eq. (9),  $\bar{x}$  represents a fixed value of  $x$  (for a given rotor design), that to be obtained by an iterative process, in order to fulfill the condition given by Eq. (11).

$$c_{m3} = c_{m6} = \bar{c}_m \tag{11}$$

Considering Eq. (11), and also due the meridional (axial) component of the absolute velocity at the inlet of the rotor,  $c_{m3}$ , be considered uniform along the blade, the first term of the right side of Eq. (9) becomes in

$$\left( \frac{c_{m3}}{\bar{c}_m} \right)_{\bar{x}}^2 = 1 \tag{12}$$

The last term of the right side of Eq. (9) is obtained through integration, resulting

$$2 \int_{\bar{x}}^x \varepsilon_6^2 \frac{dx}{x} = \left[ 2a^2 \ln x + b^2 x^2 + 4abx \right] - \left[ 2a^2 \ln x + b^2 x^2 + 4abx \right]_{\bar{x}} \tag{13}$$

The  $\bar{x}$  value is determined such that when multiplies by  $x$  the meridional velocity distribution after the rotor,  $c_{m6} / \bar{c}_m$ , given in Eq. (9), and integrated in accordance with Eq. (14), produces a value of  $\bar{c}_{m6} / \bar{c}_m$  equal one or very near this, through an iterative process.

$$\frac{\bar{c}_{m6}}{\bar{c}_m} = \frac{2}{1-x_i^2} \int_{x_i}^1 \frac{c_{m6}}{\bar{c}_m} x dx \cong 1 \quad (14)$$

where  $x_i = r_i/r_e$ . The iterative process to determine the value of  $\bar{x}$  is summarized in the following flowchart in Fig. 2:

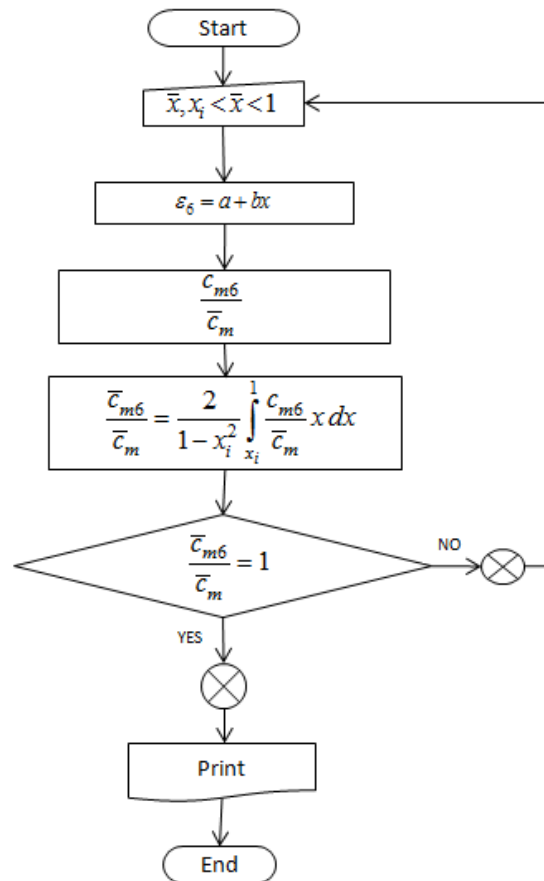


Figure 2. Flowchart for to determine  $\bar{x}$ , position along the blade where the meridional components ratio is equal to 1, for the condition non-free vortex

1) It adopts a given value of  $\bar{x}$  in the range  $x_i < \bar{x} < 1$ , preferably a value closest to the hub  $x_i$  than the tip of the blade,  $x_e = 1$ ;

2) With this value of  $\bar{x}$ , is calculated the value of  $\varepsilon_6 = a + bx$ ;  $a$  and  $b$  are constants obtained from two points on the curve  $\varepsilon_6 = \varepsilon_6(x)$ , that represents the distribution of  $\varepsilon_6$  for the free-vortex condition. The first is the referent point to the tip blade with coordinates  $(x, \varepsilon_6) = (1, \varepsilon_p)$ , where  $\varepsilon_p$  is the value of  $\varepsilon_6$  at the blade tip. The second point is the corresponding to the value of  $\bar{x}$  (arbitrary) with coordinates  $(x, \varepsilon_6) = (\bar{x}, \bar{\varepsilon})$ , where  $\bar{x}$  is the value of  $\bar{x}$  of the Item 1 above, and  $\bar{\varepsilon}$  is the value corresponding to  $\bar{x}$  removed from the free-vortex condition (Fig. 6).

3) Determining the linear dependence of  $\varepsilon_6 = \varepsilon_6(x)$ , i.e.,  $\varepsilon_6 = a + bx$ , is calculated the expression representing the velocities distribution  $c_{m6}/\bar{c}_m$ , Eq. (9), which among other parameters depends on the distribution of  $\varepsilon_6$ , which in turn depends  $\bar{x}$  (value adopted in Item 1 above).

4) Determining the velocities distribution  $c_{m6}/\bar{c}_m$  (item 3), is calculated the mean value of  $\bar{c}_{m6}/\bar{c}_m$  obtained by integration in the interval  $x_i < \bar{x} < 1$ , according to Eq. (14).

5) If  $\bar{c}_{m6}/\bar{c}_m = 1$ , was found the correct value of  $\bar{x}$ , if  $\bar{c}_{m6}/\bar{c}_m \neq 1$ , must be adopt a different value of  $\bar{x}$  and repeat the items 1 to 4 above until that  $\bar{c}_{m6}/\bar{c}_m = 1$ .

Another very important quantity in the aerodynamic design of reversible axial-flow rotor, is the mean relative fluid angle through the blade,  $\beta_\infty$ , this is obtained through the triangle of velocities of Fig. 1 and its development as well as the procedure step by step of design can be found in the work of Espinosa (2013).

$$\beta_{\infty} = \tan^{-1} \left[ \frac{\frac{1}{2} \left( 1 + \frac{c_{m6}}{c_m} \right)}{\frac{1}{\phi} - \frac{1}{2} \varepsilon_6} \right] = \tan^{-1} \left[ \frac{\frac{1}{2} \left( 1 + \frac{c_{m6}}{c_m} \right)}{\frac{2 - \phi \varepsilon_6}{2\phi}} \right] \quad (15)$$

### 3. NUMERICAL SIMULATION

The rotor used is designed for a flow of 22,7 m<sup>3</sup>/s and a rotational speed of 1760 rpm. The main geometrical characteristics are:  $D_i = 380$  mm,  $D_e = 1000$  mm and  $N_{pá} = 12$ . In the analysis of the different cases studied are considered some hypotheses as steady state and incompressible fluid and isothermal. The density and dynamic viscosity used in the simulations are  $\rho = 1,225$  kg/m<sup>3</sup> and  $\mu = 1,7894 \cdot 10^{-5}$  kg/m s, respectively. It employs the turbulence model  $k-\omega$  SST with first-order discretization.

#### 3.1 Geometry and mesh

The geometry of the rotor is made in commercial software Solid Edge ST4 ® and subsequently is exported for Icem® program, which created the computational mesh. The mesh used is non-structured with tetrahedral elements and triangular prisms. In Fig. 3, can be observed the refining conducted in the leading edge and trailing edge of the blade. This refinement is vital, because the quality of the mesh in these areas is reflected in obtaining a reliable solution.

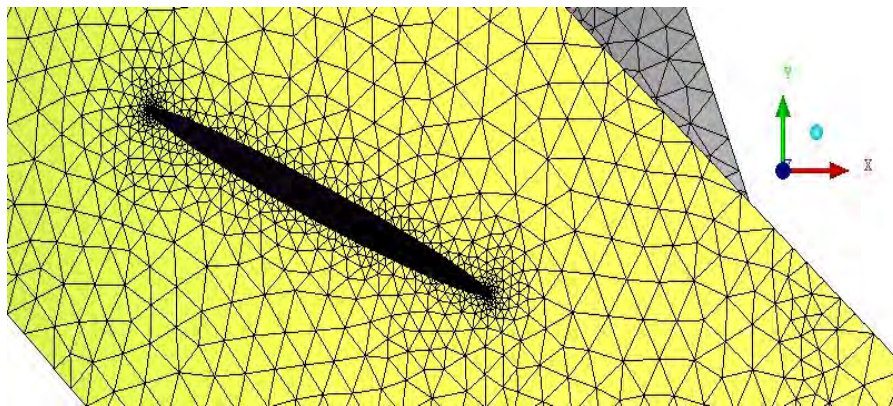


Figure 3. Refinement leading edge and trailing edge of the blade

Because the domain is repeated in each blade, it is not necessary to model this entire for the simulation, so, only the volume around one blade is meshed, which represents one-twelfth of the entire rotor. The number of elements of the mesh is 2.401.048, in Fig. 4 is shown the mesh, in this not being shown the interior elements, for a better visibility of the channel.

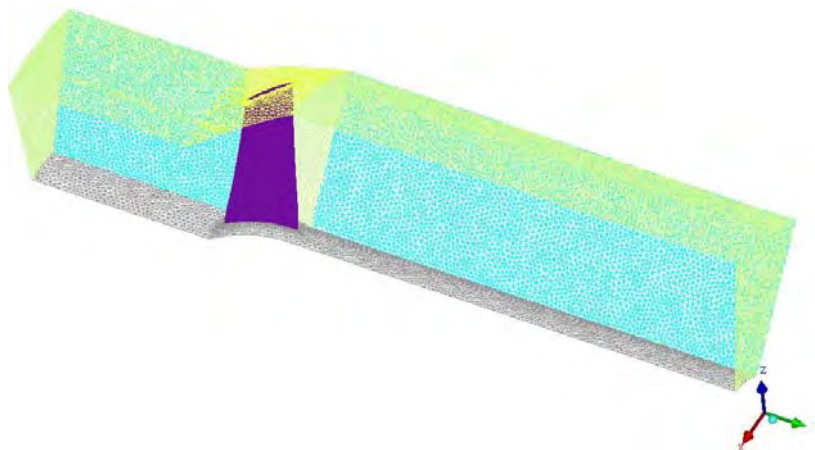


Figure 4. Computational mesh of the analyzed domain

### 3.2 Boundary conditions

The boundary conditions are imposed in the Fluent® software, which solves the governing equations for the discretized domain. On the inlet surface is fixed the condition velocity-inlet, where must be specified the initial gauge pressure, considered as 0 Pa. In the outlet surface is uses the outflow condition. Rotational periodicity condition is established in the areas which have a natural repetition. The wall boundary condition is used in solid regions where fluid flows; these surfaces may be stationary or mobile. In this study is chosen for the hub and the blade the option of rotational motion in relation to the zone of the adjacent cell, the other surfaces being treated as stationary faces. In Fig. 5 are summarized the boundary conditions mentioned above.

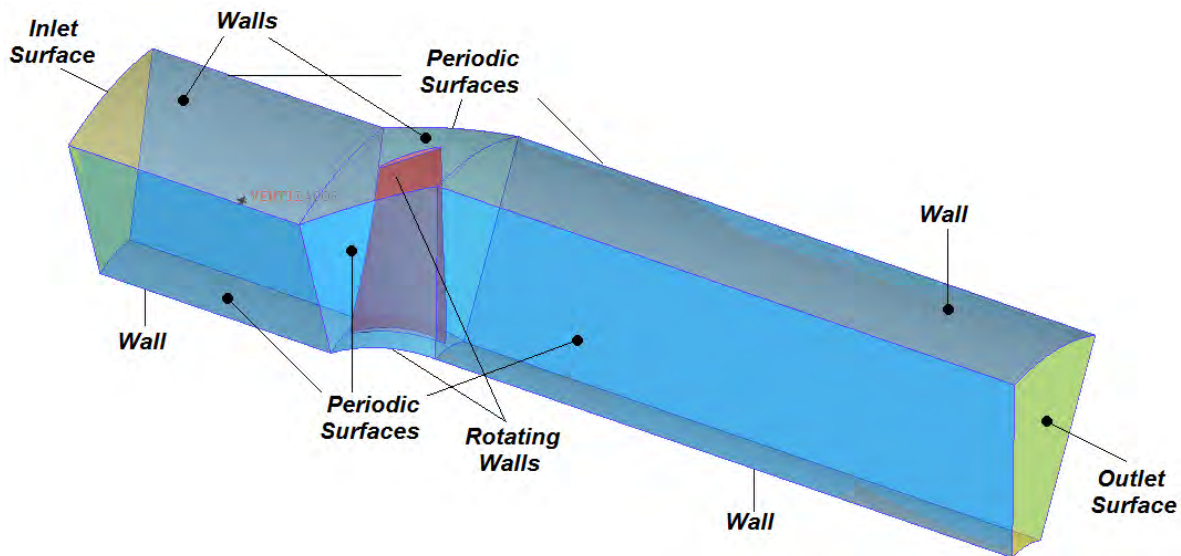


Figure 5. Boundary conditions used in the simulations

## 4. RESULTS

In the aerodynamic design procedure of the reversible rotor that uses the non free-vortex condition, was developed in this work a computational program in Fortran®, to find the correct value of  $\bar{x}$  along of the blade, unique to a particular project of rotor. The method of numerical integration (quadrature) used to solve the integral of the Eq. (14), referent to the mean value of  $c_{m6} / \bar{c}_m$ , is the Gauss-Legendre. In this technique, the number of Gaussian points ( $NPG$ ) depends on the accuracy desired and can be changed to  $NPG = 2, 3, 4, 5, 6, 7$  or  $8$ .

In the iterative procedure described in section 2.2, carried in Fortran language, for data specific of this study, was found a value of  $\bar{x} = 0,6246060$ . Thus, can be determined the constants  $a$  and  $b$  of Eq. (8), obtaining

$$\varepsilon_6 = 0,4216964 - 0,2595684x \quad (16)$$

In Fig. 6 are shown the swirl coefficients in the output of the blades along the different radial sections, by using the free-vortex methodology and the methodology of non free-vortex for the solution of radial equilibrium equation, along with the meridional velocity distribution of the flow absolute at the exit of rotor, which is represented adimensionally.

It can be seen that the proper value of  $\bar{x}$  must be positioned at the intersection of the curves representing the swirl coefficient distribution in the outlet for the vortex-free and non free-vortex. Both in this point, as in the tip of the blade ( $x = 1$ ), the meridional velocity in the output must have a value equal to one in the case of non free-vortex.

The aerodynamic performance characteristics of reversible axial rotor, are evaluated for a single rotation, 1760 rpm. In Fig. 7, are represented the curves of aerodynamic performance, total pressure, shaft power and thrust obtained from the numerical simulation in Fluent®. The layout of these is made varying the flow,  $Q$ , or axial velocity at the rotor inlet ( $c_a$  o  $c_m$ ) for 12 different operating points.

Can be appreciated that pumping limit is approximately  $12 \text{ m}^3/\text{s}$ . The number of cases simulated with flows below this limit is less, because in this region is not possible adequately represents the behavior of the fluid, for being in the unstable operation zone. Also is noted that the maximum efficiency point of the fan (69.58 %) is located in  $16,55 \text{ m}^3/\text{s}$ , and not in  $22,7 \text{ m}^3/\text{s}$ , flow for which was designed the rotor. At the design point is found in the simulations a performance of 62.06 %, a shaft power of 24,19 cv and a thrust of 807,76 N.

Espinosa, A. L. S., Oliveira, W., Ramírez, R. G. C., Quintero Y. F. G.  
 Aerodynamic Design and Determination of Performance Curves Through CFD Technicals of Axial Rotor of Reversible Jet Fan

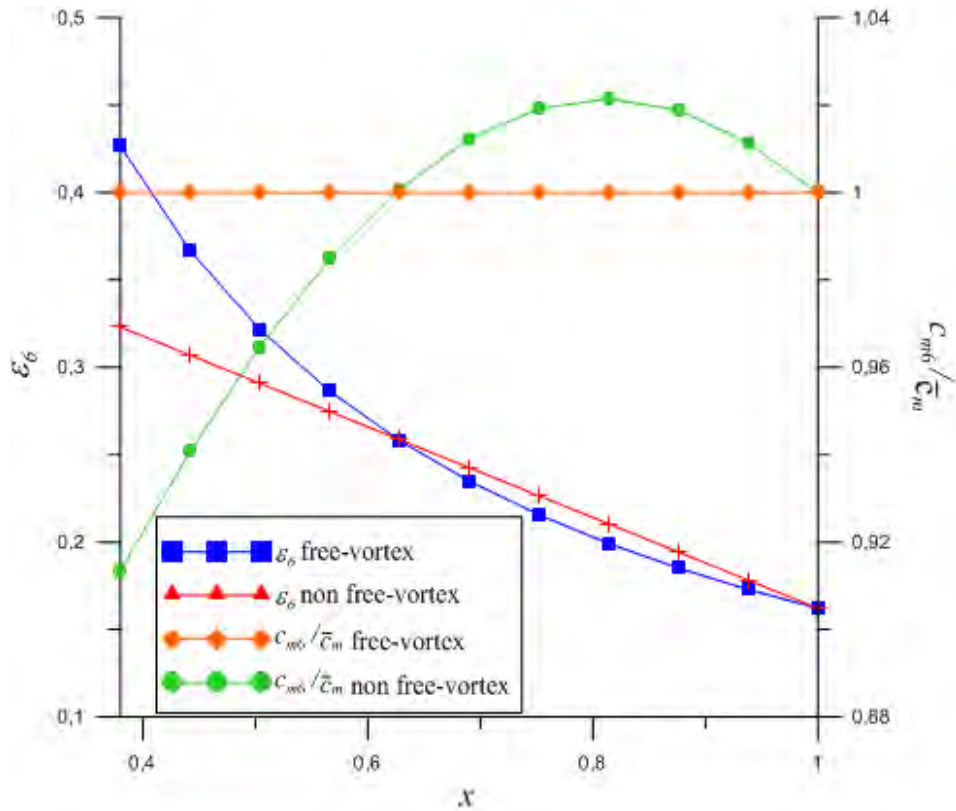


Figure 6. Swirl coefficients and meridional velocity distribution at the outlet along the length of the blade

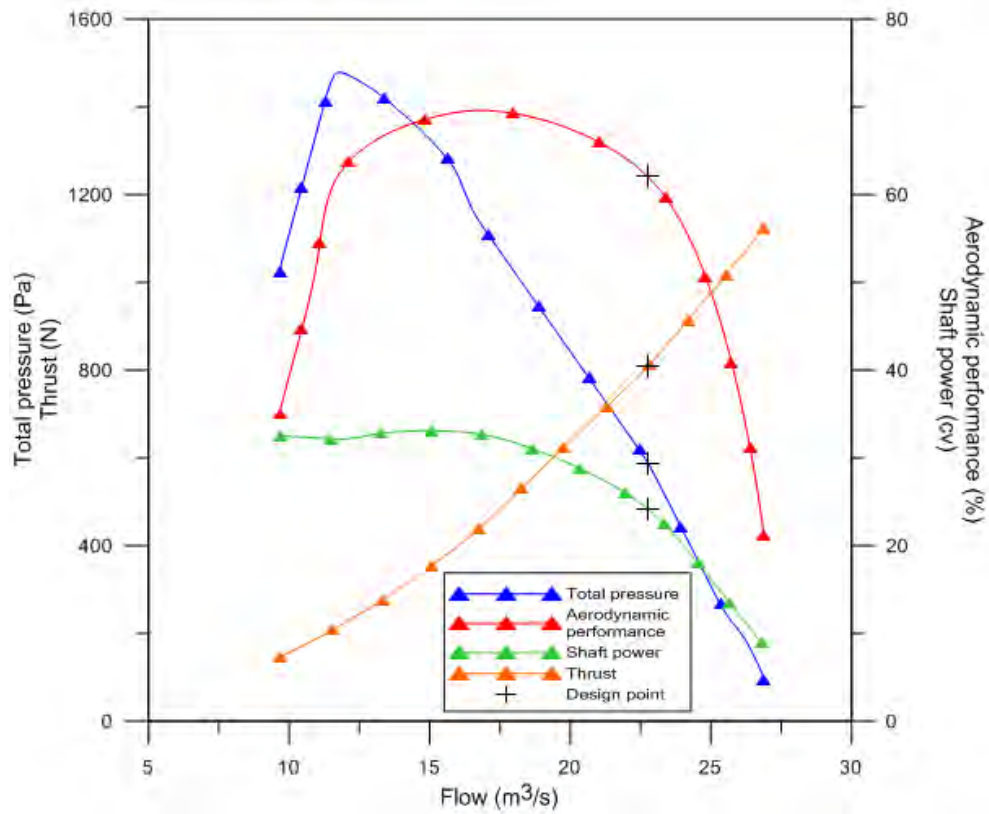


Figure 7. Characteristic curves of reversible axial rotor designed according to the condition of non free-vortex for 1760 rpm

## 5. CONCLUSIONS

Were determined the main geometric quantities of the rotor, and the most important quantities used in the aerodynamic design methodology of the blades of the reversible axial rotor, that uses the condition of non free-vortex for the solution of the radial equilibrium equation. It was found the fixed value of  $\bar{x}$  (unique to a particular rotor design) obtained through an iterative process, which is in accordance with the requirements stipulated by using the non free-vortex condition.

Were done simulations in CFD that allowed the construction of the characteristics curves of aerodynamic performance, total pressure, shaft power and thrust of axial rotor that having blades with elliptical format profiles. These curves show that the recommended working range is between 13 m<sup>3</sup>/s and 23,5 m<sup>3</sup>/s. Furthermore, is observed that the point of maximum hydraulic performance is located in 16,55 m<sup>3</sup>/s, and not in 22,7 m<sup>3</sup>/s, flow for which was designed the rotor. This difference is due to that the flow in the inlet of rotor, at a point very close to this, it is not only influenced by the presence of the blades but also by the cube of the same, especially in the closest regions to hub that in those closest to the casing. In a similar manner, the angle of the incident flow in the rotor, especially in radial sections closest to the hub, results not being the angle for the condition without shock, thus will appear shock losses (losses of incidence) where is expected the absence of such losses (design point). These facts make that decreases the performance of rotor and that its maximum value is displaced, usually, for flow rates lower than that of the design point.

## 6. ACKNOWLEDGEMENTS

The authors want to thanks the Coordination of Improvement of Higher Education (CAPES), The National Council of Technological and Scientific Development (CNPq) and The Foundation for Research Support of Minas Gerais State (FAPEMIG) for their collaboration and financial support in the development of the research work.

## 7. REFERENCES

- Ballesteros, R., Álvarez, G., Santolaria, C., Fernández, J. M. and Argüelles, K., 2002. "Análisis numérico y experimental del flujo en un ventilador de chorro". In *Proceedings of the XV Congreso Nacional de Ingeniería Mecánica*. Cadiz, Spain.
- Bleier, F. P., 1998. *Fan Handbook: Selection, Application and Design*. McGraw-Hill.
- Cordier, O., 1955. *Ähnlichkeitsbetrachtung bei Strömungsmaschinen*. VDI-Zeitschrift, Band 97, Nr. 34, S. pp 1233-1234.
- Eck, B., 1973. *Fans: design and operation of centrifugal, axial-flow and cross-flow fans*. Pergamon Press.
- Espinosa, A. L. S., Fajardo, L. C., Ramírez, R. G. C. and Oliveira, W., 2011. "Projeto aerodinâmico de rotor axial reversível de ventilador de jato", In: *Proceedings of the X Congresso Iberoamericano de Engenharia Mecânica-CIBEM10*. Oporto, Portugal.
- Espinosa, A. L. S., 2013. *Desenvolvimento de uma metodologia para o projeto aerodinâmico de rotores axiais reversíveis de ventiladores de jato de túneis rodoviários*. M.Sc. thesis, Universidade Federal de Itajubá, Brazil.
- Köktürk, T., 2005. *Design and performance analysis of a reversible axial flow fan*. M.Sc. thesis, Middle East Technical University, Turkey.
- Santolaria, C., Ballesteros, R., Blanco, E. and Parrondo, J. L., 1996. "Diseño Aerodinámico de un Ventilador de Chorro Reversible". *Información Tecnológica*, Vol. 7, N° 4, pp. 133- 140.
- Wallis, R. A., 1993. *Axial Flow Fan and Ducts*, Krieger Publishing Company.
- Yahya, S. M., 1983. *Turbines, compressors and fans*. Tata Mc Graw-Hill Publishing Company Limited.

## 8. RESPONSIBILITY NOTICE

The authors are the only responsible for the printed material included in this paper.